S. Gisinger, J. Wagner, B. Witschas 14.07.2020

***Interactive comment on* "Airborne measurements and large-eddy simulations of small-scale Gravity Waves at the tropopause inversion layer over Scandinavia" *by* Sonja Gisinger et al.**

Authors' response to the comments of the anonymous Referee #1

We appreciate the positive feedback and the valuable comments of the two anonymous reviewers #1 and #2 which we considered carefully for our revision. Thus, changes in the content of the manuscript arose, especially with respect to the momentum flux (figures and discussion). These changes became necessary due to findings we made when incorporating the reviewers' comments. We spent some more time on the momentum flux calculations and the assessment of their sensitivity and uncertainty and managed to find a way of analyzing the momentum fluxes in measurements and simulations such that they provide robust vertical profiles in terms of their trend. The range of uncertainty for the quantitative momentum flux values is also included. Previously, we were not aware of the sensitivity of the averaged momentum flux, however, also thanks to the reviewer comments, we consider the sensitivity of the momentum flux calculation on the background removal and leg length in the revised momentum flux analysis and in the discussion of the manuscript. Below you will find a detailed explanation of the changes in the manuscript as well as the point-to-point answers to the review comments. All modified figures and one new figure are also attached at the end of this document.

Momentum flux

In the framework of the revision of the paper manuscript, we tried to quantify the influence of the reflected and trapped waves in the troposphere on the momentum flux (MF) profile (and also derived the MF profiles for the realistic simulation runs 5 and 6). By doing so, we realized that the determination of the perturbations u' and w' was not properly or rather not extensively enough described in the previous version of the manuscript. Moreover, during this analysis it turned out that the resulting MF profile is sensitive with respect to the background fit and the length and start/end points of the flight leg (not only for the measurements but also for the most idealized case of interfacial waves on a boundary layer inversion). By separating the leg into 3 segments for the measurements, we had already shown that there is a clear variability. But only after doing more detailed analyses and sensitivity test, we found out that we had drawn incomplete conclusions for the MF profile of the interfacial waves. The positive MF in the vicinity of the TIL is actually not due to the interfacial waves but due to the longer waves (>30 km) that are influenced by the TIL. The leg-averaged MF of the interfacial waves is close to zero (a detailed explanation is given below). The former downstream segment 3 was longer than segments 1 and 2, and thus, longer waves remained in u' and w' of segment 3. Considering this, we have carefully revised the parts of the manuscript that deal with the MF profiles.

The most important points/changes are:

+ We use spectral filters to determine u' and w' for different wave classes (long, intermediate, and short waves, i.e. mainly mountain waves, reflected and trapped waves in the troposphere, and interfacial waves). We separate the wave classes based on their horizontal wavelengths as seen in

the wavelet power spectra. long waves > 6 km and short waves < 6 km for the boundary layer simulations (Run 1, 2). Long waves > 30 km, intermediate waves 10 km to 30 km, and short waves < 10 km for the measurements and the TIL/no-TIL simulations (Run 5, 6). The advantage of the spectral filter is that the wavelengths contained in u' and w' are clearly defined. For the usual background fit, the wavelengths vary with the length of the leg. This is not appropriate for the purpose of our analyses. A similar separation of wave classes can be found in Georgelin and Lott 2001.

additional reference:

Georgelin, M. and Lott, F.: On the transfer of momentum by trapped lee waves: Case of the IOP 3 of PYREX, J. Atmos. Sci., 58, 3563–3580, https://doi.org/10.1175/1520-0469(2001)058<3563:OTTOMB>2.0.CO;2, 2001a.

+ Boundary layer simulations: we show the MF profile for the two wave classes in Fig. 13. When the MF is averaged for the whole domain, the MF profiles of the long waves and the short waves show a distinctive kink at the altitude of the inversion (Fig. 13e). This is not found when the inversion is absent (Fig. 13a). When the MF is averaged for the downstream region, the resulting MF of the interfacial waves depends on the exact start/end points of the downstream region with respect to the wave phase. This is because the interfacial waves show alternating positive and negative fluxes downstream of the mountain (Fig. 13b). In contrast to upward propagating mountain waves (Fig. 13d), the phase shift between u' and w' is -90° for interfacial below the inversion (Fig. 13c) and changes to +90° right above the inversion (not shown). When the MF is averaged over a downstream region that only contains full wave cycles, the resulting MF is zero for well-established and totally trapped interfacial waves (Fig. 13e). When the start/endpoints of the downstream region are chosen such that waves are partly included, the MF can be neg. (pos.) right below the inversion and pos. (neg.) above the inversion. The sign of the MF depends on the cutting location in the wave cycles, i.e. depends on if more neg. (pos.) MF is included in the average (Fig. 13b). This happened in Fig. 13 for the first version of the manuscript.

+Measurements and realistic simulations: A thousand sub-legs are created as such that their start (end) point is fixed at the westernmost (easternmost) point of the measurements and the length of the leg is stepwise extended eastward (westward) by 1 km starting with a minimum length of 200 km and going up to 700 km, i.e. the full leg length. This is done to incorporate the sensitivity of the leg-averaged MF with respect to the start/end points of the leg and the corresponding unequal sampling of updrafts and downdrafts as already suggested and analyzed in a similar way by Brown (1983). We additionally found differences in the MF from lidar and HALO in-situ data at 7.8 km altitude, although one hardly can determine differences in u and w between lidar and HALO in-situ data. In particular, the difference in w is 0.0 ± 0.2 m s^{-1} on average. In the end, the given standard deviation accounts for these uncertainties in the MF profile being a worst case estimate with sub-legs included which have lengths shorter than λ_{MAX} /2 with theoretically λ_{MAX} ≈ 700 km. The fact that the mean MF profile computed from the set of sub-legs is close to the MF profile averaged for the full leg distance [-300, 400 km], which has the largest likelihood to capture the full wave cycles of the wave packages, supports that the sub-legs are chosen in a proper way (new Fig. 16).

additional reference:

Brown, P. R. A.: Aircraft measurements of mountain waves and their associated momentum flux over the British Isles, Quarterly Journal of the Royal Meteorological Society, 109, 849–865, https://doi.org/10.1002/qj.49710946211, https://rmets.onlinelibrary.wiley.com/doi/abs/10.1002/qj.49710946211, 1983.

+Measurements vs realistic simulations: The wave field is much more complicated and complex compared to the idealized boundary layer case. The MF profiles can be distinguished for the three wave classes defined above. The most prominent feature is the kink reaching positive values for the long waves between 8-km and 9-km altitude. Negative fluxes of the same magnitude are found below. The mean MF at 7.8-km altitude of the DWL and the HALO in-situ data differs but within the range of the uncertainty. It is worth mentioning that the uncertainty in the MF from the in-situ data is largest at this altitude and larger than the uncertainty derived for the DWL data. This means the MF from in-situ at this altitude could be biased to MF of larger magnitude due to localized peaks in ρu'w' along the leg. The intermediate and short scale waves show similar MF profiles with small undulations around zero. The leg-averaged momentum flux of the long waves is positive (around −0.05 Pa) at 13.3-km altitude which could be a hint for wave reflection in the stratosphere or a stratospheric source creating downward propagating GWs.

For the simulations, the MF profiles of the three wave classes clearly distinguish from each other (Fig. 16). The pronounced kink in the MF profiles of the long waves (>30 km) and the short waves (<10km) in the altitude range of 7 km to 9 km is a clear feature of the effect of the TIL and not visible in the no-TIL simulation (Fig. 16a). The amplitudes of the long (i.e. mountain waves) and intermediate waves (i.e. reflected and trapped waves in the troposphere) and their resulting MF are overestimated compared to the observations (Fig. 6 and Fig. 15f-i). The MF is overall negative for these simulations but close to zero for the short waves. These findings are most likely an effect of the 2-dimensional model setup. Interestingly, the MF of the long waves shows a larger magnitude in the simulation without TIL (Fig. 16a) compared to the simulation with TIL (Fig. 16b). The MF of the intermediate waves shows an opposite behavior, i.e. smaller in magnitude in the simulation without TIL. This change in MF between the two simulations suggests stronger reflection of the MWs at the TIL. This is a finding that is in agreement with findings from the single mountain simulations.

1. General Comments

This is an excellent paper that melds analysis of data from recent field campaigns with idealized numerical modelling to obtain insight into apparent interfacial waves in the tropopause inversion layer. I find it to be well written and enlightening from a scientific point of view, and it deserves publication in ACP. Nonetheless, I do have several (mostly minor) comments and questions.

We thank the reviewer for this positive feedback and his/her valuable comments and questions that helped to improve the manuscript.

2. Specific Comments

• In RF08 FL1, there is also a region of positive MF at λ = 30-40 km and x = 200-250 km that is almost equal in magnitude to the region of negative MF perturbations at λ = 40-50 km and x = 120 km. The latter region is attributed to vertically propagating waves in the text, but is there any explanation for the positive MF region?

Taking into account the new findings for the leg-averaged MF profile at different scales, we could add for the positive MF region:

…Positive MF for the long waves is found in RF08 FL1 at 220 km distance which could be caused by partial reflection of these waves at the TIL.

…

…

The most prominent feature is the kink reaching positive values for the long waves between 8-km and 9-km altitude. Negative fluxes of the same magnitude are found below. This strengthens the previous assumption that waves are partially reflected at the TIL.

• How long are the simulations run for? Are they at approximately steadystate?
Run1 and Run2: 96min, Run3: 190min, Run4: 96min
The initial disturbance created by the mountain during the initialization of the simulations has moved far enough downstream in the region of interest and the simulations have reached quasi steady state by that time.

Run5 &6: 977min (~16h) as it takes longer for the initial disturbance to reach the border of the 1008-km large domain. In contrast to the single mountain simulations, these simulations having more complex topography do not reach quasi steady state due to continuous interaction of waves from the different mountain peaks, tropospheric trapped waves, and interfacial waves.

We added this information to Sec. 3.2 and added an extra column in Table 1:

… The total integration time for these simulations is between 96 and 190 minutes. The initial disturbance created by the mountain during the initialization of the simulations has moved far enough downstream in the region of interest and the simulations have reached quasi steady state by that time. Table 1 summarizes the relevant initial parameters and total integration time for the different model runs.

… The total integration time for these simulations is 16~hours. This is longer than for the other set of simulations because it takes longer for the initial disturbance to reach the border of the larger domain. In contrast to the single mountain simulations, these simulations having more complex topography do not reach quasi steady state due to continuous interaction of waves from the different mountain peaks, tropospheric trapped waves, and interfacial waves.

• The initial profiles for the more realistic idealized simulations appear that they may be capable of supporting trapped waves due to the wind shear in the troposphere. There appear to be trapped-wave-like structures in the troposphere in both the no-TIL and TIL cases, which may also be leaking into the stratosphere, particularly in the TIL inversion case where there is an even larger Scorer parameter in the inversion. Where do these perturbations appear in the wavelet analysis? Could leakage of waves from the troposphere complicate the attribution of perturbations in the TIL to interfacial waves?
These tropospheric trapped waves are seen in the wavelet analyses at scales of 10-30 km horizontal wavelengths (Fig. 6, Fig. 15). In the revised version, we demonstrate that it is possible to separate the interfacial waves from the tropospheric trapped waves based on their scales. We revised the analysis of the measurements and simulations and computed the MF for three different wave classes (> 30km, 10 km to 30 km, and < 10 km). The MF of the interfacial waves and of the reflected and trapped waves in the troposphere is similar and varies around zero (Fig. 10). Trapped waves in the troposphere are known to have leg-averaged MFs of around zero (Woods and Smith, 2010; Georgelin and Lott, 2001).

• When discussing waves with wavelength of ~ 8 km, it is very difficult to gain an appreciation of the structure with the aspect ratio in the vertical velocity plots. It would be nice to stretch out the horizontal axis a bit more for ease of interpretation.
We agree that the aspect ratio was not the best choice in the first draft of the manuscript. We changed the aspect ratio and alignment of the panels for Figs. 8, 9, and 14.

• It might be nice to show one or two example soundings (with θ) for the idealized cases outlined in Table 1, which would help illustrate the exact setup of the inversion.
Done, we added the four θ-profiles to Fig. 11.

• Line 45: The sentence beginning here is oddly worded. I think it would be better to make clear that "they" here refers to the fundamental characteristics of the hydrostatic approximation. At first reading it initially seems like "they" refers to the findings.
Done, we changed the sentence as suggested.

…The fundamental characteristics of the hydrostatic approximation are the absence of a mechanism which allows a wave to propagate horizontally and the consequent upward propagation of energy directly above the obstacle, regardless of the horizontal extent of the generating terrain…

• Line 146: The ρ_0 of the Boussinesq approximation is not actually defined in the text.
ρ_0=1.225 kg/m^3, we added this information to Sec. 2.3.

• Line 175: It might be useful to note that the "critical horizontal wavelength" is also referred to as the Scorer parameter, especially since the Scorer parameter is referenced elsewhere in the text. It may also be helpful to have the equation for the Scorer parameter written in the paper as well.
Done, we added the definition of the Scorer parameter to the introduction and the definition of the critical horizontal wavelength to Sec. 3.1.1.
…

$$\ell^2(z) = \frac{N^2(z)}{U^2(z)} - \frac{\partial^2 U(z)/\partial z^2 + \partial U(z)/\partial z/H}{U(z)} - \frac{1}{4H^2} \quad (1)$$

…
The critical horizontal wavelength $(= 2\pi/\ell)$ …

• Line 194: I think it would be good to have a citation for alternating momentum fluxes being an indication of reflected and trapped waves.
We added the reference of Woods and Smith 2010 and updated Fig. 13 which now shows that alternating momentum fluxes indicate trapped waves due to the phase relationship of u' and w'. We added the cross-reference to the section in which Fig. 13 is described.
…
This alternating pattern is an indication for reflected and trapped waves (Woods and Smith 2010, see also Sec. 3.2).
…
• Line 280: "Interfacial small 280 scale waves are absent in the troposphere below the TIL (Fig. 15i) and in the case of no TIL (RUN 5, Fig. 14c and Fig. 15a, c)." For the no-TIL simulation, are you referencing below the would-be TIL or above or both? The referenced figures imply above, but text seems to imply either below or both.
We clarified the description accordingly.

…Small scale interfacial waves are absent in the case of no TIL (Fig. 14a, c). They are only found in the TIL (Fig. 15f, h) but not below (Fig. 15g, i)…

3. Technical Corrections
• Line 304: Second word should be "were" instead of "where"
Done.
• Line 305: Extra "to" in "range of to"
This paragraph was revised according to the results of the updated MF analyses.

… In the lower stratosphere, the leg-averaged MF was found to be positive (around 0.05 Pa). This is in contrast to the findings during DEEPWAVE where no positive leg-averaged MF was found in the lower stratosphere above New Zealand ([Fig. 5b in (Smith et al., 2016)]. However, analyses in Smith et al. (2016) are limited to waves having scales < 150 km and at least in ground-based lidar data

downward propagating waves were frequently observed in wintertime in the stratosphere above New Zealand (Kaifler et al., 2017).

additional reference:

Kaifler, N., Kaifler, B., Ehard, B., Gisinger, S., Dörnbrack, A., Rapp, M., Kivi, R., Kozlovsky, A., Lester, M., and Liley, B.: Observational indications of downward-propagating gravity waves in middle atmosphere lidar data, Journal of Atmospheric and Solar-Terrestrial Physics, 162, 16 – 27, https://doi.org/10.1016/j.jastp.2017.03.003, 2017.

Modified and new figures

- modified (new aspect ratio):

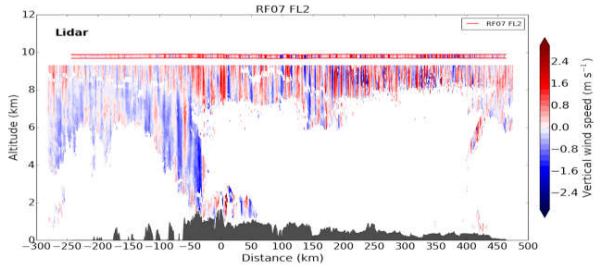

Figure 8. Vertical winds along flight leg RF07 FL2 measured by the DWL and in-situ instruments (marked by red horizontal lines) at flight level by the DLR Falcon.

- modified (new aspect ratio):

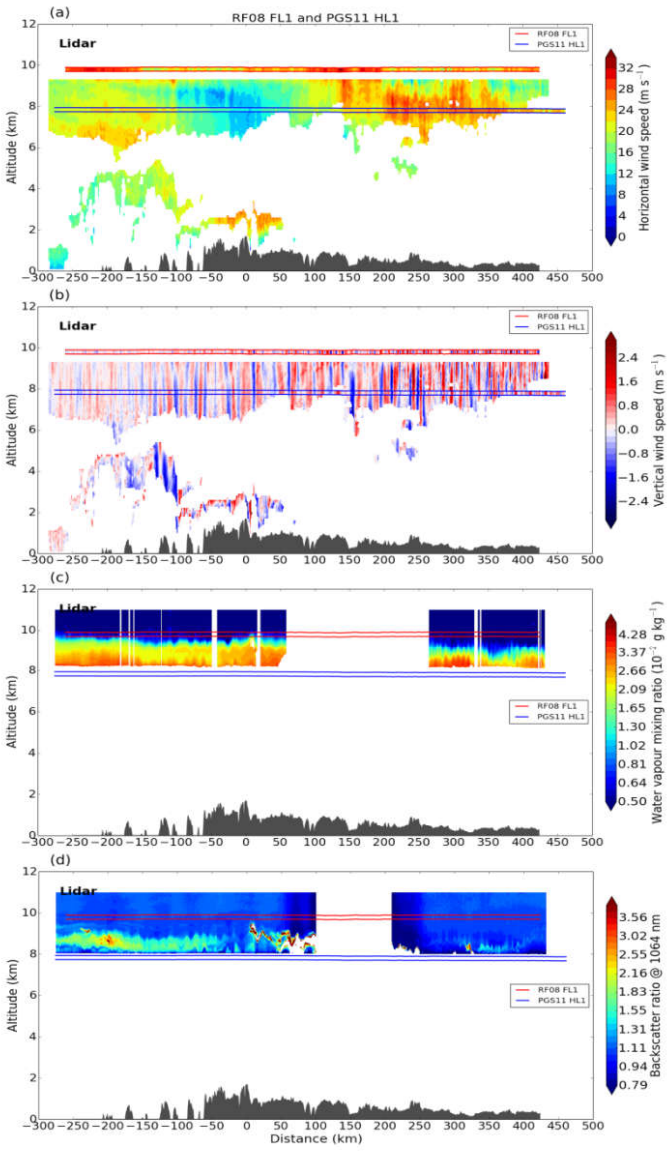

Figure 9. DWL measurements of (a) horizontal wind speed and (b) vertical wind speed and WALES measurements of (c) water vapour mixing ratio and (d) lidar reflectivity along flight leg RF08 FL1/PGS11 HL1 combined with corresponding in-situ measurements of HALO and DLR Falcon at flight level (marked by blue and red horizontal lines).

- modified (revised data analysis):

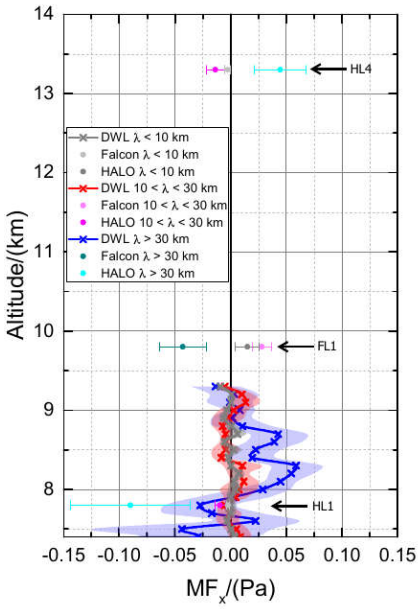

Figure 10. Leg-averaged momentum fluxes as mean for varying leg length (solid) with standard deviation (shading, error bars) along flight leg RF08 FL1 obtained from DWL (×) and in-situ measurements (●) which include also PGS11 HL1 and HL4. Three wave classes are colour coded and bold black line separates positive and negative fluxes.

- modified (additional panels):

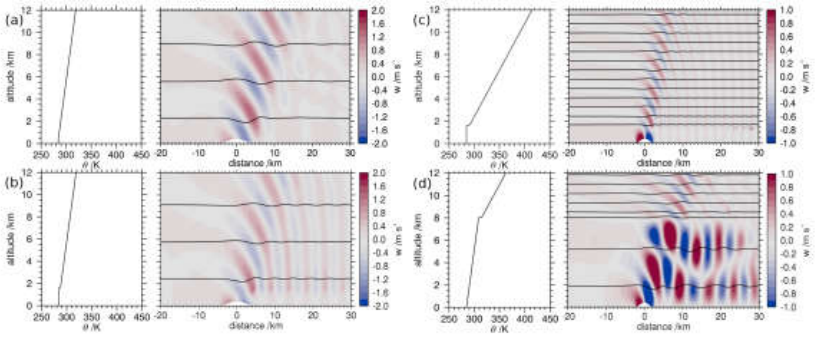

Figure 11. Potential temperature and vertical velocity of the idealized simulations of the cases with (a) a neutral boundary layer without inversion and $N_U = 0.01\ \mathrm{s}^{-1}$ (RUN 1), (b) a neutral boundary layer with an inversion of 3.3 K and $N_U = 0.01\ \mathrm{s}^{-1}$ (RUN 2), (c) a neutral boundary layer with an inversion of 6.6 K and $N_U = 0.02\ \mathrm{s}^{-1}$ (RUN 3), and (d) a stable troposphere ($N = 0.01\ \mathrm{s}^{-1}$) with a TIL of 6.6 K and $N_U = 0.02\ \mathrm{s}^{-1}$ (RUN 4).

- modified (revised data analysis, new panels):

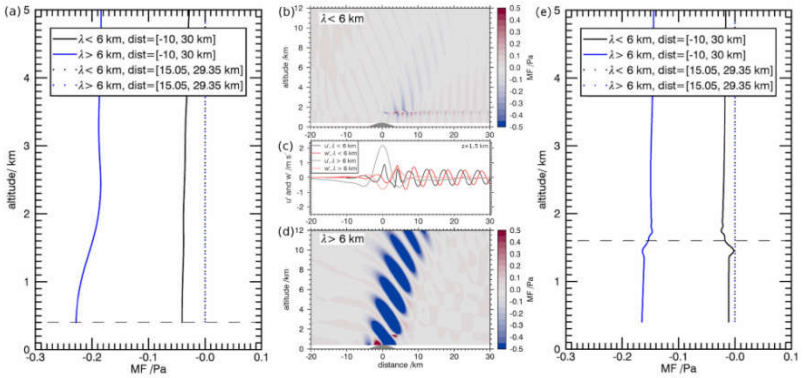

Figure 13. Momentum flux (profiles) for (a) RUN 1 without boundary layer inversion (Figs. 11a, 12a) and (b,d,e) Run 2 with boundary layer inversion (Figs. 11b, 12c) for two wave classes (horizontal wavelength smaller or larger 6 km). Profiles show averages for the full distance (solid) and for the downstream distance (dotted); horizontal dashed lines marks the top of the boundary layer. (c) shows u' and w' for the two wave classes at 1.5 km altitude revealing their phase relationship right below the inversion, i.e.- 90° for interfacial waves (black and red lines).

- modified (new aspect ratio):

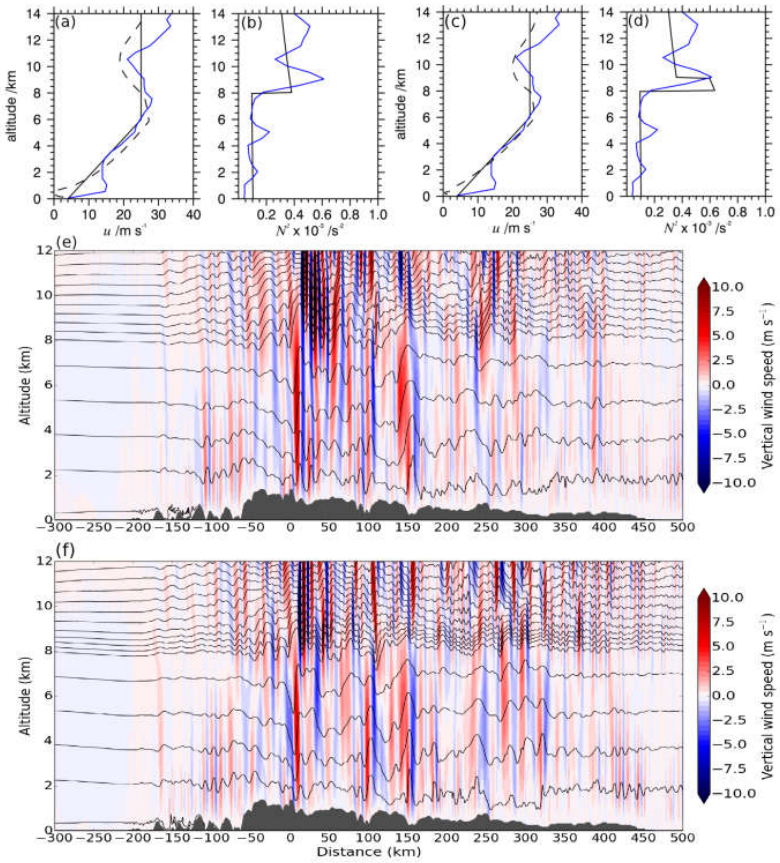

Figure 14. Initial profiles (black solid) and vertical velocity for the simulations with more realistic terrain without TIL (a, b, e; RUN 5) and with TIL (c, d, f; RUN 6). The initial profiles approximate the background conditions over southern Scandinavia on 28 January 2016 (blue profiles show the Stavanger radiosonde data). Negative shear above the tropopause establishes in the course of the simulations (a, d; black dashed, time = 16 h, distance = −150 km).

- new figure:

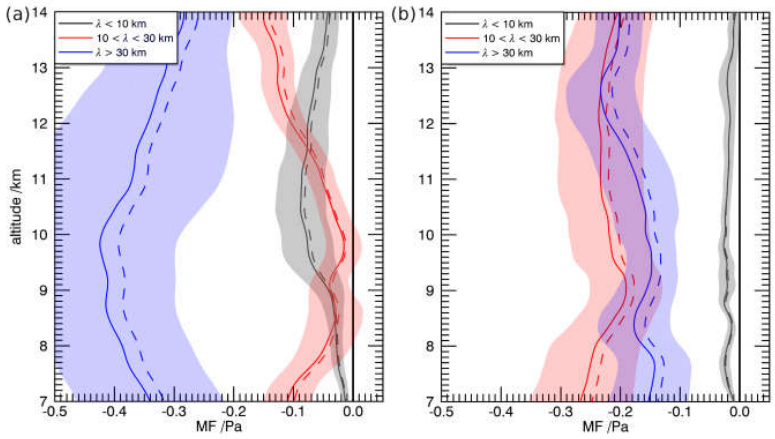

Figure 16. Averaged momentum fluxes for (a) RUN 5 (no TIL) and (b) RUN 6 (TIL) as mean for varying leg length (solid) with standard deviation (shading) and for the full leg distance [-300, 400 km] (dashed). Three wave classes are color coded and bold black line separates positive and negative fluxes